

Catalysis Science & Technology

Accepted Manuscript



This is an *Accepted Manuscript*, which has been through the Royal Society of Chemistry peer review process and has been accepted for publication.

Accepted Manuscripts are published online shortly after acceptance, before technical editing, formatting and proof reading. Using this free service, authors can make their results available to the community, in citable form, before we publish the edited article. We will replace this *Accepted Manuscript* with the edited and formatted *Advance Article* as soon as it is available.

You can find more information about *Accepted Manuscripts* in the [Information for Authors](#).

Please note that technical editing may introduce minor changes to the text and/or graphics, which may alter content. The journal's standard [Terms & Conditions](#) and the [Ethical guidelines](#) still apply. In no event shall the Royal Society of Chemistry be held responsible for any errors or omissions in this *Accepted Manuscript* or any consequences arising from the use of any information it contains.



Journal Name

ARTICLE

Kinetic Analysis of Aqueous-phase Cyclodehydration of 1,4-Butanediol and Erythritol over a Layered Niobium Molybdate Solid Acid

Received 00th January 20xx,
Accepted 00th January 20xx

DOI: 10.1039/x0xx00000x

www.rsc.org/

Atsushi Takagaki^{a,*}

Aqueous-phase reactions are desirable for the transformation of biomass-derived species because the use of water is inherently environmentally friendly. Cyclodehydration of C4 diols in aqueous solution was examined using a variety of water-tolerant solid acids including H-type zeolites (H-ZSM5, H-mordenite, H-beta), Amberlyst-15 ion-exchange resin, niobic acid and layered HNbMoO₆. Cyclodehydration of 1,4-butanediol (HO-CH₂CH₂CH₂CH₂-OH) and erythritol (HO-CH₂CH(OH)CH(OH)CH₂-OH) proceeded on three of the Brønsted solid acids, HNbMoO₆, H-ZSM5 and Amberlyst-15. Although HNbMoO₆ showed moderate activity for 1,4-butanediol dehydration, it exhibited the highest activity for erythritol dehydration. Kinetic analysis indicated that 1,4-butanediol and erythritol dehydration over HNbMoO₆ followed a Tamaru-type mechanism with two successive irreversible steps. A statistical mechanics analysis of the pre-exponential factor gave good agreement with experimental results, in which the pre-exponential factor for erythritol dehydration was much larger than that for 1,4-butanediol dehydration. Both erythritol and 1,4-butanediol could be intercalated in the interlayer spaces of the oxide. The expansion of the interlayer spaces for erythritol was, however, much larger than that for 1,4-butanediol. This improvement of accessibility is considered to be responsible for the higher reactivity of erythritol.

Introduction

Chemical reactions in aqueous solution have attracted much attention in the field of green and sustainable chemistry because water is a safe, harmless, and non-flammable solvent. A variety of bio-derived compounds such as alcohols, ethers, carboxylic acids, carbohydrates, and sugar alcohols are highly soluble in water, because its polarity and high dielectric constant enhance interactions. Heterogeneous acid catalysts, which are reusable and easily separable, offer the opportunity to reduce environmental impact. For this reason, water-tolerant solid acids such as zeolites (high-silica HZSM-5¹ and Sn-beta²), sulfonated carbon materials (amorphous carbon³ and graphene oxide⁴), transition metal oxides (niobic acid⁵ and ceria⁶), immobilized heteropolyacids,⁷ and metal-organic frameworks⁸ have been widely explored.

Transformation of biomass-derivatives in water are important processes in biorefineries.⁹⁻¹¹ Hydrolysis of cellulose occurs in water, which affords glucose, a representative platform molecule. Glucose is further transformed into sugar alcohols, erythritol (C4) and sorbitol (C6) in water *via* fermentation and hydrogenation, respectively. The products of dehydration of these sugar alcohols are high value-added

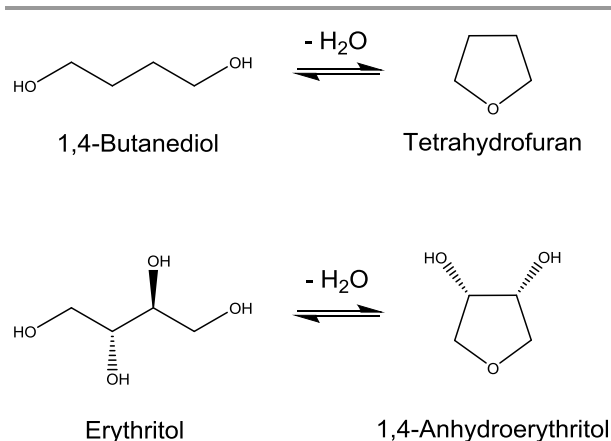
chemicals, 1,4-anhydroerythritol, 1,4-anhydro-sorbitol (1,4-sorbitan), and 1,4:3,6-dianhydro-sorbitol (isosorbide), which are widely used for synthesis of polymers, surfactants, cosmetics and medicines.^{12,13}

The layered metal oxide, HNbMoO₆, which consists of two-dimensional [NbMoO₆]⁻ anion sheets composed of NbO₆ and MoO₆ octahedra,¹⁴ is one of the most promising water-tolerant solid acids.¹⁵ A variety of substrates including alcohols, ketones and sugars can be intercalated, resulting in high performance for Friedel-Crafts alkylation, acetalization and hydrolysis reactions.¹⁵

Recently, the aqueous-phase cyclodehydration of sorbitol has been demonstrated with a variety of water-tolerant solid acids including the zeolite H-ZSM5, the ion-exchange resin Amberlyst-15 and the metal oxides niobic acid and HNbMoO₆.¹⁶ It was found that the layered compound HNbMoO₆ exhibited the highest selectivity toward 1,4-sorbitan (1,4-anhydro-sorbitol) with high conversion, which was attributed to the intercalation of sorbitol within the interlayers. This reaction proceeds via 1,4-cyclodehydration, and the same reaction is applicable for the synthesis of 1,4-anhydroerythritol from erythritol (Scheme 1). This study compares the aqueous-phase 1,4-cyclodehydration of erythritol using various solid acids, and examines the reaction mechanisms for the most active catalysts. The 1,4-cyclodehydration of 1,4-butanediol to tetrahydrofuran (THF) was also examined as a test reaction to investigate the effect of the two additional hydroxyl groups in erythritol on the 1,4-cyclodehydration.

^a Department of Chemical System Engineering, School of Engineering, The University of Tokyo, 7-3-1 Hongo, Bunkyo-ku, Tokyo 113-8656, Japan.
atakagak@chemsys.t.u-tokyo.ac.jp

Electronic Supplementary Information (ESI) available: Calculation of lack of mass transfer limitation. See DOI: 10.1039/x0xx00000x



Scheme 1 Reactions of 1,4-cyclodehydration of 1,4-butanediol and erythritol.

Experimental

Catalyst preparation: Layered HNbMoO_6 was obtained from LiNbMoO_6 according to a procedure described in the literature.¹⁴ Briefly, the layered LiNbMoO_6 was prepared by calcination of a stoichiometric mixture of Li_2CO_3 (Wako, >99.0%), Nb_2O_5 (Wako, 99.9%) and MoO_3 (Wako, >99.0%) at 853 K for 24 hours with one intermediate grinding step. A proton-exchange reaction was carried out by shaking 2.0 g of the lithium precursor in 200 mL of 1 M HNO_3 solution at room temperature for 1 week with one intermediate exchange with HNO_3 solution. After that, the product was washed with 800 mL of distilled water and dried in air at 373 K.

The substances H-ZSM5 (nominal Si/Al = 45, JRC-Z-5-90H), H-mordenite (nominal Si/Al = 10, JRC-Z-HM20), H-beta (nominal Si/Al = 12.5, JRC-Z-HB25), niobic acid ($\text{Nb}_2\text{O}_5 \cdot n\text{H}_2\text{O}$, HY-340) and Amberlyst-15 were also studied. The zeolites H-ZSM5, H-mordenite and H-beta were provided by the Japan Reference Catalyst Division of the Catalysis Society of Japan. Niobic acid $\text{Nb}_2\text{O}_5 \cdot n\text{H}_2\text{O}$ was supplied by Companhia Brasileira de Metalurgia e Mineração (CBMM), and Amberlyst-15 was obtained from Sigma-Aldrich Inc.

The acid amounts of zeolites and niobic acid were determined by temperature-programmed desorption of ammonia (NH_3 -TPD) using a TPD-1-AT instrument (MicrotracBEL) equipped with a quadrupole mass spectrometer. A quantity of 20 mg sample was heated at 673 K (zeolites) or 473 K (niobic acid) for 1 h under helium flow, exposed to NH_3 at 373 K for adsorption, and finally heated at 10 K min^{-1} . The acid amounts of HNbMoO_6 were determined by ^{31}P magic angle spinning nuclear magic resonance (MAS NMR) using trimethylphosphine oxide (TMPO) as a probe molecule as described elsewhere.¹⁵ The NH_3 -TPD measurement for HNbMoO_6 was not appropriate because of difficulty of intercalation of NH_3 in gas phase.¹⁵

Dehydration of 1,4-butanediol and erythritol: A quantity of 1.0 mmol of 1,4-butanediol (Wako, >98.0%) or 0.41 mmol of *meso*-erythritol (TCI, >99.0%) with 50 mg of solid acid catalyst was stirred in 3 mL water in a glass reactor vessel (Ace glass pressure tube). The concentration of 1,4-butanediol is 0.33 mol L^{-1} ($2.0 \times 10^{20} \text{ cm}^{-3}$) and that of *meso*-erythritol is 0.14 mol

L^{-1} ($8.2 \times 10^{19} \text{ cm}^{-3}$). The reactor vessel was placed in an oil bath at 393 – 443 K. The heating time was 0.5 – 15 h. The reactants and products were analysed by high performance liquid chromatography (HPLC; LC-2000 plus, JASCO) equipped with a differential refractive index detector (RI-2031 plus, JASCO) using Aminex HPX-87H column ($300 \times 7.8 \text{ mm}$, 4.8 MPa, 323 K, flow rate: 0.5 mL min^{-1} , eluent; $10 \text{ mM H}_2\text{SO}_4$). The retention times of 1,4-butanediol, tetrahydrofuran, *meso*-erythritol and 1,4-anhydroerythritol were determined to be 25.5, 41.0, 13.7 and 17.7 min, respectively. The reaction rate is defined as the moles of product produced per liter of solution per hour ($\text{mol L}^{-1} \text{ h}^{-1}$). The turnover frequency (s^{-1}) is calculated from the reaction rate by normalization with the number of acid sites per liter of solution. X-ray diffraction patterns of the samples were obtained with a diffractometer operated at 40 kV and 100 mA, using Cu-K α radiation (RINT-2700, Rigaku).

Results and Discussion

Table 1 lists results for the cyclodehydration of 1,4-butanediol and *meso*-erythritol (1,2,3,4-butanetetraol) using a variety of solid acid catalysts. The performance of the catalysts was evaluated at low substrate concentrations and low product yields to be in the kinetic regime. Lack of mass transfer limitations was verified from the Weisz-Prater criteria, and the calculations are summarized in Supplementary information (see ESI). Three water-tolerant Brønsted acids, the oxide HNbMoO_6 , the sulfonated resin Amberlyst-15 and the zeolite H-ZSM5 showed catalytic activities for cyclodehydration of 1,4-butanediol with excellent selectivity toward tetrahydrofuran whereas other acidic zeolites (H-mordenite and H-beta) and niobic acid ($\text{Nb}_2\text{O}_5 \cdot n\text{H}_2\text{O}$) were inactive.

Table 1 Aqueous-phase cyclodehydration of 1,4-butanediol and *meso*-erythritol using solid acid catalysts.

Catalyst	Acid amount /mmol g ⁻¹	1,4-Butanediol ^a		<i>meso</i> -Erythritol ^b	
		Conv./%	Sel./% ^c	Conv./%	Sel./% ^d
HNbMoO_6	1.9 ^e	19	>99	28, 70 ^f	>99, 90 ^f
$\text{Nb}_2\text{O}_5 \cdot n\text{H}_2\text{O}$	0.3 ^g	7	0	0	-
Amberlyst-15	4.8 ^h	44	>99	14	>99
H-ZSM5	0.2 ^g	50	>99	37	59
H-mordenite	1.1 ^g	11	0	0	-
H-beta	1.0 ^g	3	0	0	-

^a Reaction conditions: 1,4-Butanediol (1.0 mmol), catalyst (50 mg), water (3 mL), 413 K, 3 h. ^b Reaction conditions: *meso*-Erythritol (0.41 mmol), catalyst (50 mg), water (3 mL), 433 K, 18 h. ^c Selectivity of tetrahydrofuran. ^d Selectivity of 1,4-anhydroerythritol. ^e Determined by ^{31}P MAS NMR using trimethylphosphine oxide. ^f *meso*-Erythritol (1 mmol), catalyst (50 mg), water (1.5 mL), 443 K, 30 h. ^g Determined by NH_3 -TPD. ^h Ref 17.

The order of reactivity of the active acid catalysts is indicated below. These catalysts had moderately high conversions in 3 h of reaction and very high selectivity:

1,4-Butanediol dehydration: H-ZSM5 > Amberlyst-15 > HNbMoO_6

The three catalysts also showed activities for cyclodehydration of erythritol, while the other solid acids tested were inactive. However, the results for the cyclodehydration of erythritol were different from those of 1,4-butanediol. H-ZSM5 showed the highest conversion (36%), but its selectivity toward 1,4-anhydroerythritol was rather low (59%) and other unidentified compounds (oligomerization products) observed as by-products. In contrast, HNbMoO₆ and Amberlyst-15 afforded excellent selectivity toward the corresponding anhydro product (> 99%). HNbMoO₆ exhibited the highest yield among solid acids for erythritol dehydration. The high selectivity was maintained even at high conversion (conversion 70%, selectivity 90%). The order of reactivity based on the product yield is given below. In a separate study, the same order of reactivity was observed for the cyclodehydration of sorbitol where H-ZSM5 again gave low selectivity.¹⁶

Erythritol dehydration: HNbMoO₆ > H-ZSM5 > Amberlyst-15

1,4-Butanediol dehydration

Figure 1 shows plots of initial reaction rate against initial 1,4-butanediol concentrations over the three active solid acids, HNbMoO₆, Amberlyst-15 and H-ZSM5 at 413 K. Initial substrate concentrations were in the range of 0.06–3.3 mol L⁻¹. The reaction rates over Amberlyst-15 and H-ZSM5 are not directly proportional to the reactant concentration, but instead curved downward. The rate for HNbMoO₆ has only a slight curvature, but still can be described by the same kinetic schemes.

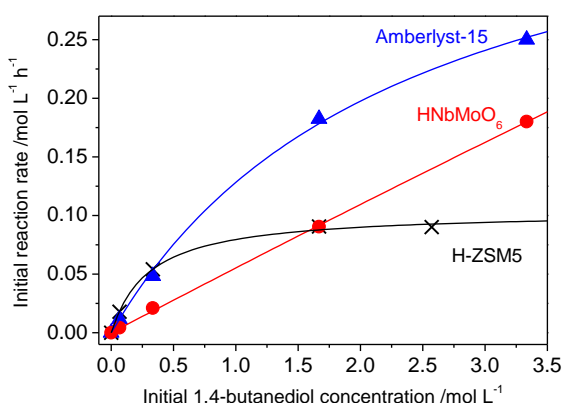


Figure 1 Plots of initial reaction rate against initial 1,4-butanediol concentrations using HNbMoO₆, Amberlyst-15 and H-ZSM5 (Reaction conditions: 1,4-butanediol (0.2 – 10 mmol), catalyst (50 mg), water (3 mL), 413 K).

A first candidate sequence for the transformation of a reactant R to a product P through an adsorbed intermediate R* is the following.



The well-known Langmuir-Hinshelwood treatment gives:

$$r = (S) \frac{a(R)}{[1 + b(R)]} \quad (3)$$

where $(S) = (*) + (R^*)$ is the total concentration of sites (units), $a = k_2 K_1$, and $b = K_1$, where k_2 is the rate constant for the second step and $K_1 = k_1/k_{-1}$ is the adsorption equilibrium constant for the first step. The symbol (R) is conventionally the concentration of the reactant with laboratory units of mol/L, but in a formal kinetic treatment it would be the activity, which is dimensionless because the concentration is divided by the standard state concentration of 1 mol/L. Here the standard state concentration will be incorporated into the rate constant and the conventional units of (R) will be retained. Details will be provided below. If the sites are mostly bare, $1 \gg K_1(R)$, and the rate expression becomes:

$$r = (S) k_2 K_1 (R) \quad (4)$$

An alternative candidate that considers two irreversible steps ($k_{-1} = 0$) results in $r = r_1 = r_2$. As far as the authors are aware, this approach was first applied by Tamaru and coworkers for the kinetics of ammonia decompositions.^{18,19} This gives $r = k_1(R)(*) = k_2(R^*)$, and again using $(S) = (*) + (R^*)$ results in the same expression (3) as before. Only the meaning of the parameters is changed with $a = k_1$ and $b = k_1/k_2$. If adsorption is rate-determining $k_2 \gg k_1(R)$ and the expression becomes:

$$r = (S) k_1 (R) \quad (5)$$

Table 2 lists the fitted reaction rate parameters for the cyclodehydration of 1,4-butanediol at various temperatures (393 – 423 K). The common rate expression fits well at each temperature, with high values of regression coefficient. The fitted parameters are also reasonable at first glance. Figure 1 shows that the rate on HNbMoO₆ displays an almost linear dependence on concentration and so its parameter b is close to zero. The figure also shows that the rate on H-ZSM5 reaches a plateau so that the b parameter is large, while the rate on Amberlyst-15 rises monotonically, so that the b parameter is intermediate in value.

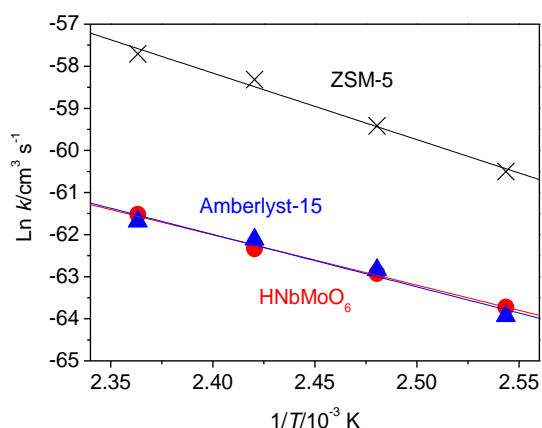
The results of H-ZSM5 and Amberlyst-15 can be analysed by the Langmuir-Hinshelwood kinetics (Eqn 4). On the contrary, the results of HNbMoO₆ will be analysed by the Tamaru kinetics, in which the rate expression is given by $r = (S) k_1 (R)$ (Eqn 5), because the Langmuir-Hinshelwood kinetics, in which the rate expression is $r = (S) k_2 K_1 (R)$ (Eqn 4), loses significance (reaction rate r becomes zero) when the parameter $b = K_1$ is almost zero.

Table 2 Kinetic fits for the cyclodehydration of 1,4-butanediol (BDO) over HNbMoO₆, Amberlyst-15 and H-ZSM5

Catalyst	Temp. K	Parameter <i>a</i>		Parameter <i>b</i>		R ^{2a}
		10 ⁻³ L (mol BDO) ⁻¹ s ⁻¹	10 ⁻²⁷ cm ³ s ⁻¹	L (mol BDO) ⁻¹ cm ³	10 ⁻²⁷ cm ³	
HNbMoO ₆	393	0.13	0.21	0.05	0.91	0.995
	403	0.28	0.47	0.05	0.88	0.999
	413	0.51	0.85	0.03	0.43	0.999
	423	1.2	1.9	0.02	0.31	0.999
Amberlyst-15	393	0.10	0.17	0.13	2.2	0.999
	403	0.31	0.51	0.25	4.2	0.994
	413	0.64	1.1	0.43	7.1	0.999
	423	0.98	1.6	0.42	7.0	0.992
H-ZSM5	393	3.2	5.3	2.8	46	0.996
	403	9.5	16	4.3	72	0.997
	413	28	47	3.3	55	0.998
	423	52	87	2.7	45	0.994

^a Regression coefficient

Figure 2 shows Arrhenius plots for the cyclodehydration of 1,4-butanediol over the three solid acids. Activation energies and pre-exponential factors were obtained from these plots. Activation energies were estimated to be 99, 104 and 132 kJ mol⁻¹ for HNbMoO₆, Amberlyst-15 and H-ZSM5, respectively. Pre-exponential factors showed considerable differences among the three catalysts. These were estimated to be 3.5 × 10⁻¹⁵, 1.1 × 10⁻¹⁴ and 1.7 × 10⁻⁹ cm³ s⁻¹ for HNbMoO₆, Amberlyst-15 and H-ZSM5, respectively. H-ZSM5 showed high values of pre-exponential factor, suggesting that 1,4-butanediol can access the active sites of the zeolite. In contrast, HNbMoO₆ showed low values of the pre-exponential factor. This possibly suggests that the initial interaction of the butanediol with the surface of the HNbMoO₆ is involved in the rate-determining step. Namely, reaction occurs rapidly after intercalation.

**Figure 2** Arrhenius plots for cyclodehydration of 1,4-butanediol over HNbMoO₆, Amberlyst-15 and H-ZSM5.

The pre-exponential factor may be estimated from transition state theory. For an adsorption process the pre-

exponential factor, A, of the rate constant k_1 in equation (5) is given by:

$$A = \frac{k_B T}{h} \exp\left(\frac{\Delta S^\ddagger}{R}\right) = \frac{k_B T}{h} \frac{Q''}{Q'} \quad (6)$$

In the equations ΔS^\ddagger is the activation entropy, R is the gas constant, k_B is Boltzmann's constant, h is Planck's constant, T is the temperature, Q'' the overall partition function of the activated complex, and Q' the overall partition function of the reactant. The term $k_B T/h$ is known as the universal frequency and has a value of $8.50 \times 10^{12} \text{ s}^{-1}$ for the average temperature of 408 K for the 1,4-butanediol reactions, which spans the region of 393-423 K. The overall partition functions have contributions from translational, rotational, vibrational, and electronic partition functions, identified by the appropriate subscripts below. Usually, the electronic contribution is small and will not be considered in this analysis. The overall partition function ratio can also be expressed as the difference of the entropy contributions of each mode between the reactant and the transition state.

$$\frac{Q''}{Q'} = \frac{q_r'' q_v'' q_e''}{q_r' q_v' q_e'} = \exp\left(\frac{\Delta S}{R}\right) \quad (7)$$

In preparation for the estimation of the pre-exponential factors it is useful to calculate the various partition functions in Eqn. 7. This is carried out using standard formulas,²⁰ and the results are summarized in Table 3.

The use of these formulas is mostly straightforward as described in physical chemistry textbooks. However, there is one aspect that is usually not covered and merits mention, and that is the characteristic dimensions in the translational partition functions. These partition functions make use of the characteristic volume (V) for 3-d translation, the corresponding area (A) for 2-d translation, and the relevant length (L) for 1-d translation. Whereas in the gas-phase the characteristic volume would be given by RT/P , in the liquid-phase use is made of the density (ρ), whose units are converted using the molecular weight (MW_{BD}) and Avogadro's number (NA) to obtain $V = MW_{BD}/\rho N_A$. The corresponding area is obtained from $A = V^{2/3}$, and length from $L = V^{1/3}$. Note that the values for V, A, and L are physically realistic. Thus, the volume of $1.47 \times 10^{-22} \text{ cm}^3$ is larger than the volume of the molecule, a reasonable space for occupancy. Likewise the area of $2.78 \times 10^{-15} \text{ cm}^2$ compares with the area for a monolayer of 10^{-15} cm^2 , and the length of $5.28 \times 10^{-8} \text{ cm}$ is larger than the lateral dimensions of BD. Partition functions for rotation in three and one dimension utilize the moment of inertia, I, which is obtained from the literature for butanediol.²² Partition functions for vibration utilize the normal modes, which are also obtained from the literature.²³ Only the most intense 10 lines were used out of a total of $3N+5 = 53$ ($N=16$ atoms in butanediol).



Journal Name

ARTICLE

Table 3. Calculation of partition functions and entropies for butanediol

Type	Degrees of freedom	Partition function q	Value	Entropy	Value J/ mol K
Translational q_t^3	3	$(2\pi mk_B T)^{3/2}/h^3$	$1.32 \times 10^{27} \text{ cm}^{-3}$	$R \ln[Vq_t^3] + 3/2R$	114
Translational q_t^2	2	$(2\pi mk_B T)/h^2$	$1.20 \times 10^{18} \text{ cm}^{-2}$	$R \ln[Aq_t^2] + R$	75.7
Translational q_t^1	1	$(2\pi mk_B T)^{1/2}/h$	$1.10 \times 10^9 \text{ cm}^{-1}$	$R \ln[Lq_t^1] + 1/2R$	37.9
Rotational q_r^3	3	$\frac{\sqrt{\pi}(8\pi^2 I k_B T)^{3/2}}{\sigma h^3}$	1.43×10^5	$R \ln[q_r^3] + 3/2R$	111
Rotational q_t^1	1	$\frac{(8\pi^2 I k_B T)^{1/2}}{\sigma h}$	2.72×10^1	$R \ln[q_r^1] + 1/2R$	31.6
Vibrational q_v	1	$\frac{1}{1 - e^{-u}}$	3.29×10^{-5} ⋮ 0.150	$\sum R \left[\frac{u}{e^u - 1} - \ln(1 - e^{-u}) \right]$	6.2

$T = 408 \text{ K}$. BD = Butanediol. $MW_{BD} = 90.12 \text{ g/mol}$. $\rho = 1.02 \text{ g/cm}^3$. $S_{liq}^0 = 223.4 \text{ J mol}^{-1}\text{K}^{-1}$ [ref 21]

$V = MW_{BD}/\rho N_A = 90.12 \text{ g/mol}/(1.02 \text{ g cm}^{-3})(6.02 \times 10^{23} \text{ mol}^{-1}) = 1.47 \times 10^{-22} \text{ cm}^3$

$A = V^{2/3} = (1.47 \times 10^{-22} \text{ cm}^3)^{2/3} = 2.78 \times 10^{-15} \text{ cm}^2$

$L = V^{1/3} = (1.47 \times 10^{-22} \text{ cm}^3)^{1/3} = 5.28 \times 10^{-8} \text{ cm}$

$c = 3.00 \times 10^{10} \text{ cm s}^{-1}$ $h = 6.6261 \times 10^{-27} \text{ cm}^2 \text{ g s}^{-1}$ $k_B = 1.3807 \times 10^{-16} \text{ cm}^2 \text{ g s}^{-2} \text{ K}^{-1}$

$I_a = 50 \text{ g \AA}^2 \text{ mol}^{-1}$, $I_b = 280 \text{ g \AA}^2 \text{ mol}^{-1}$, $I_c = 390 \text{ g \AA}^2 \text{ mol}^{-1}$ [ref 22]

$I = (I_a I_b I_c)^{1/3} = 176 \text{ g \AA}^2 \text{ mol}^{-1} = 176 \times (10^{-8} \text{ cm/\AA})/6.02 \times 10^{23} \text{ mol}^{-1} = 2.92 \times 10^{-38} \text{ g cm}^2$

$\bar{\nu} = 3670, 3650, 3480, 1090, 1075, 1060, 1045, 1020, 995, 965 \text{ cm}^{-1}$ [ref 23]

$$u = \frac{h\nu}{k_B T} = \frac{h\bar{\nu}c}{k_B T}$$

$$\sum R \left[\frac{u}{e^u - 1} - \ln(1 - e^{-u}) \right] = [3.29 \times 10^{-5} + 3.51 \times 10^{-5} + 6.13 \times 10^{-5} + 0.105 + 0.110 + 0.115 + 0.129 + 0.138 + 0.150]$$

The partition functions can also be used to calculate entropies, and these are reported in Table 4. The sum of the 3-d translation, 3-d rotation, and vibrational contributions to entropy amount to $231 \text{ J mol}^{-1}\text{K}^{-1}$, which come close to the reported value for butanediol in the liquid phase of $223 \text{ J mol}^{-1}\text{K}^{-1}$,²¹ with the discrepancy probably due to hindered motion in the liquid phase.

With the partition functions evaluated it is possible to calculate the pre-exponential factors. Considering first

HNbMoO_6 at the top of Table 4, the pre-exponential factor is the smallest, suggesting loss of considerable entropy in forming the activated complex. For an activated complex that is immobile $q_t'' = 1$ and for a reagent which is free to translate in three dimensions $q_{t-3}''' = (2\pi mk_B T/h^2)^{3/2} = 1.32 \times 10^{27} \text{ cm}^{-3}$ (Table 3) so the pre-exponential factor A is estimated as follows.

$$A = \frac{k_B T}{h} \frac{Q^\ddagger}{Q} = (8.50 \times 10^{12} \text{ s}^{-1}) \frac{1}{1.32 \times 10^{27} \text{ cm}^{-3}} = 6.44 \times 10^{-15} \text{ cm}^3 \text{ s}^{-1} \quad (8)$$

This is close to the experimental value for HNbMoO₆ of $3.5 \times 10^{-15} \text{ cm}^3 \text{ s}^{-1}$, so no further assumptions about the other degrees of freedom are needed. The adsorption of 1,4-butanediol can be viewed as occurring by the loss of all translational motion in forming the activated complex, but with retention of vibrational and rotational states.

Table 4 Activation energies and pre-exponential factors of cyclodehydration of 1,4-butanediol

Order ^a	Catalyst	E_a kJ mol ⁻¹	Exp. A cm ³ s ⁻¹	Transition state	Calc. A cm ³ s ⁻¹	R^2 ^b
3	HNbMoO ₆	99	3.5×10^{-15}	Immobile	6.44×10^{-15}	0.996
2	Amberlyst-15	104	1.1×10^{-14}	1-d trans.	3.74×10^{-14}	0.969
1	H-ZSM5	132	1.7×10^{-9}	2-d trans.	2.15×10^{-11}	0.989

T = 393-423K ^a Activity order ^b Regression coefficient for Arrhenius plot

Considering Amberlyst-15, the second entry in Table 4, the pre-exponential factor is slightly larger than that of HNbMoO₆, suggesting the activated complex will have more degrees of freedom. For an activated complex with one degree of translational freedom $L(2\pi mk_B T/h^2)^{1/2} = (5.28 \times 10^{-8} \text{ cm})(1.10 \times 10^9 \text{ cm}^{-1}) = 5.81 \times 10^1$, the pre-exponential factor is estimated to be:

$$A = \frac{k_B T}{h} \frac{Q^\ddagger}{Q} = (8.50 \times 10^{12} \text{ s}^{-1}) \frac{(5.81 \times 10^1)}{(1.32 \times 10^{27} \text{ cm}^{-3})} = 3.74 \times 10^{-14} \text{ cm}^3 \text{ s}^{-1} \quad (9)$$

This is reasonably close to the experimental value for Amberlyst-15 of $1.1 \times 10^{-14} \text{ cm}^3 \text{ s}^{-1}$, so no further analysis will be undertaken.

Considering HZSM-5, the third entry in Table 4, the pre-exponential factor is the largest, indicating the most mobile activated complex. For a complex with two degrees of translational motion $A(2\pi mk_B T/h^2) = (2.78 \times 10^{-15} \text{ cm}^2)(1.20 \times 10^{18} \text{ cm}^{-2}) = 3.34 \times 10^3$, and the pre-exponential factor is estimated to be:

$$A = \frac{k_B T}{h} \frac{Q^\ddagger}{Q} = (8.50 \times 10^{12} \text{ s}^{-1}) \frac{(3.34 \times 10^3)}{(1.32 \times 10^{27} \text{ cm}^{-3})} = 2.15 \times 10^{-11} \text{ cm}^3 \text{ s}^{-1} \quad (10)$$

Although deviating more than the other pre-exponential factors, this is reasonably close to the experimental value for HZSM-5 of $1.7 \times 10^{-9} \text{ cm}^3 \text{ s}^{-1}$, so again no further calculations will be undertaken.²⁴

Examination of all the entries in Table 4 shows that the calculated pre-exponential values are close to the experimental values with just consideration of the loss of translational degrees of freedom. Better agreement can be obtained by considering rotational and vibrational degrees of

freedom. Examination of the kinetic parameters (Table 3) shows that the highest activation energy is accompanied by the highest pre-exponential factor. This is a manifestation of the compensation effect.^{25,26} It is evident that the pre-exponential factor has the biggest influence on the rate.

Erythritol dehydration.

The same experiments were carried out for cyclodehydration of erythritol. Figure 3 shows plots of initial reaction rate against initial erythritol concentrations over the three catalysts at 443 K. The results were substantially different from those of 1,4-butanediol dehydration. The reaction rates of HNbMoO₆ were higher than those of Amberlyst-15 and H-ZSM5. The order of reactivity was HNbMoO₆ > Amberlyst-15 > H-ZSM5, and remained unchanged within the range of initial substrate concentrations tested (0.33 – 3.3 mol L⁻¹). Table 5 lists the fitted reaction rate parameters for the cyclodehydration of erythritol at various temperatures (413 – 443 K). The rate on HNbMoO₆ increased monotonically with small value of parameter *b*. On the contrary, the parameters *b* for Amberlyst-15 and H-ZSM5 were almost zero, indicating that these reactions followed simple first-order equations, of the Tamaru mechanism. As before, these are consistent with adsorption being rate-determining, with subsequent reactions being fast.

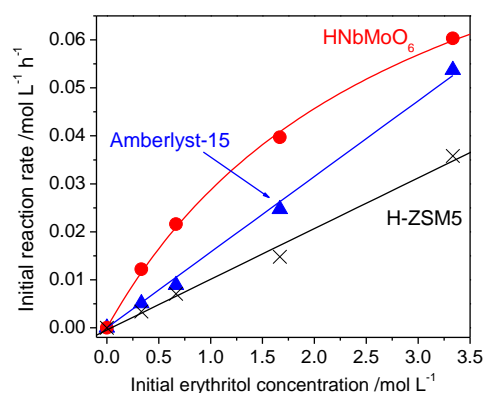


Figure 3 Plots of reaction rate against initial erythritol concentrations using HNbMoO₆, Amberlyst-15 and H-ZSM5 (Reaction conditions: meso-erythritol (1 – 10 mmol), catalyst (50 mg), water (3 mL), 443 K).

Table 5 Kinetic fits for the cyclodehydration of erythritol (EOH) over HNbMoO₆, Amberlyst-15 and H-ZSM5

Catalyst	Temp. K	Parameter <i>a</i>		Parameter <i>b</i>		R ^{2a}
		10 ⁻⁵ L (mol EDO) ⁻¹ s ⁻¹	10 ⁻²⁸ cm ³ s ⁻¹	L (mol EDO) ⁻¹	10 ⁻²⁵ cm ³	
HNbMoO ₆	413	2.5	0.42	0.07	1.2	0.979
	423	6.8	1.1	0.20	3.3	0.996
	433	15	2.5	0.24	3.9	0.999
	443	34	5.6	0.35	5.7	0.999
Amberlyst-15	413	0.44	0.07	0.05	0.91	0.997
	423	1.2	0.20	0	0	0.999
	433	2.7	0.44	0	0	0.995
	443	5.5	0.91	0	0	0.997
H-ZSM5	413	8.3	1.4	0.06	0.10	0.997
	423	22	3.6	0.06	1.1	0.988
	433	45	7.5	0	0	0.995
	443	87	14	0	0	0.990

^a Regression coefficient

Figure 4 shows Arrhenius plots for erythritol dehydration, and Table 6 lists activation energies and pre-exponential factors. Activation energies for erythritol dehydration were estimated to be 131, 128 and 119 kJ mol⁻¹ for HNbMoO₆, Amberlyst-15 and H-ZSM5, respectively. The activation energy and pre-exponential factor over HNbMoO₆ for erythritol dehydration were higher than those for 1,4-butanediol dehydration. This suggests that erythritol is strongly adsorbed to the active sites of HNbMoO₆ and the adsorbed amount is high, which follows a Langmuir-type mechanism. Compared to the results of 1,4-butanediol dehydration, the activation energy over Amberlyst-15 for erythritol dehydration was also higher than those for 1,4-butanediol dehydration, suggesting that the presence of the two additional hydroxyl groups makes it the reaction more difficult. The pre-exponential factor for erythritol dehydration over H-ZSM5 was lower than those for 1,4-butanediol dehydration. The pore sizes of ZSM5 zeolite are 0.54 × 0.56 nm²⁷ and the molecular size of tetrahydrofuran is estimated to be 0.41 nm.²⁸ Thus, 1,4-butanediol dehydration is easily carried out in the pore of the zeolite. The additional hydroxyl groups in erythritol likely hinder the formation of the corresponding product, 1,4-anhydroerythritol, and this led to the lower pre-exponential factor and a reaction dominated by adsorption in H-ZSM5 for erythritol dehydration. Pore size alone is not the primary determinant of activity. The H-mordenite zeolite has pores of size 0.65 nm while beta zeolite has pores of size 0.66 - 0.56 nm, which are bigger than those of ZSM5, yet both are inactive. Probably the pore shape and arrangement of acid sites are important in determining activities, with a tighter geometry being favourable for the cyclization reaction.

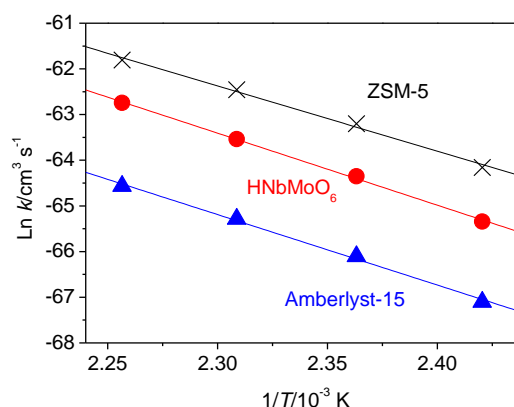
Only a brief transition state calculation will be given here for HNbMoO₆, the most active catalyst. Using the methodology used for 1,4-butanediol, with a median temperature of 428 K ($k_B T/h = 8.92 \times 10^{12} \text{ s}^{-1}$) the loss of one degree of translational freedom gives a $q_t'' = A(2\pi m k_B T/h^2) =$

$(2.69 \times 10^{-15} \text{ cm}^2)(1.31 \times 10^9 \text{ cm}^{-2}) = 4.63 \times 10^3$, and for a reagent which is free to translate in three dimensions $q_{t-3}''' = (2\pi m k_B T/h^2)^{3/2} = 2.25 \times 10^{27} \text{ cm}^{-3}$, the pre-exponential factor A is estimated to be as follows.

$$A = \frac{k_B T}{h} \frac{Q''}{Q'''} = (8.92 \times 10^{12} \text{ s}^{-1}) \frac{4.63 \times 10^3}{2.25 \times 10^{27} \text{ cm}^{-3}} = 1.83 \times 10^{-11} \text{ cm}^3 \text{ s}^{-1} \quad (11)$$

This is in reasonable agreement with the experimental value of $1.6 \times 10^{-12} \text{ cm}^3 \text{ s}^{-1}$ (Table 6).

The larger value of the pre-exponential factor for erythritol over 1,4-butanediol can be ascribed to the larger mobility of the activated complex, due to the accessibility in the layered structure (*vide infra*). The analysis presented here shows that the experimentally obtained rate parameters have physically realistic values, and gives support to the mechanistic scheme presented.

**Figure 4** Arrhenius plots for cyclodehydration of erythritol over HNbMoO₆, Amberlyst-15 and H-ZSM5.**Table 6** Activation energies and pre-exponential factors of cyclodehydration of erythritol

Catalyst	<i>E_a</i> /kJ mol ⁻¹	<i>A</i> /cm ³ s ⁻¹	R ^{2a}
HNbMoO ₆	131	1.6×10^{-12}	0.999
Amberlyst-15	128	1.3×10^{-13}	0.997
H-ZSM5	119	1.5×10^{-13}	0.995

^a Regression coefficient for Arrhenius plot

Intercalation of 1,4-butanediol and erythritol into HNbMoO₆

In our previous studies, we proposed that intercalation of substrates into layered HNbMoO₆ is responsible for its high catalytic activity.^{15,16} The intercalation can be monitored by the shifts in basal spacing of the layered oxide using x-ray diffraction (XRD). To confirm the possibility, HNbMoO₆ was immersed in aqueous solutions of 1,4-butanediol or erythritol at room temperature overnight, then filtered off and dried at 373 K. Figure 5 shows the results of XRD patterns before and

after immersion of 1,4-butanediol or erythritol. It was confirmed from the high angle region that the in-plane crystal structure remained unchanged. In contrast, notable shifts of the peak corresponding to the basal spacing were observed for the samples immersed in 1,4-butanediol or erythritol. The basal spacing were estimated to 1.65 and 1.79 nm for 1,4-butanediol and erythritol, respectively. Because the basal spacing of the fully dehydrated HNbMoO_6 is 1.08 nm,¹⁴ expansions were 0.57 and 0.71 nm for 1,4-butanediol and erythritol, respectively. Since the distances between the two terminal OH groups of 1,4-butanediol and erythritol were calculated to be 0.76 and 0.77 nm, respectively, these reactants would be intercalated in monolayer conformations with inclination angles of 48° (1,4-butanediol) and 68° (erythritol) to the basal plane. The former value is consistent with the case of α -zirconium phosphate (47.6°).²⁹ The presence of the two additional OH groups in erythritol changed the interlayer spacing, which might be responsible for different reactivity between 1,4-butanediol and erythritol dehydration. The expansion of layers would improve adsorption of erythritol, resulting in higher pre-exponential factor for erythritol dehydration than that for 1,4-butanediol.

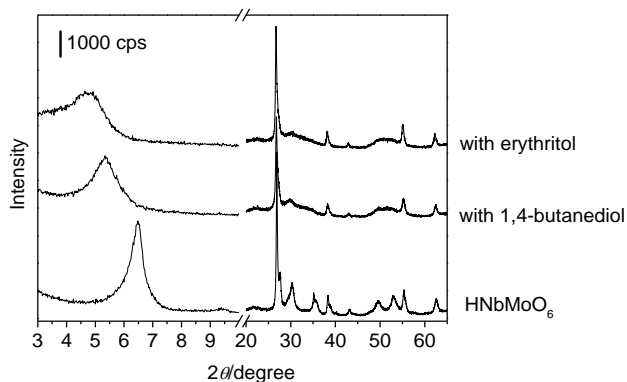


Figure 5 XRD patterns for hydrated HNbMoO_6 , and HNbMoO_6 after immersion in aqueous solution containing 1,4-butanediol and erythritol.

Conclusions

HNbMoO_6 , H-ZSM5 and Amberlyst-15 were found to catalyse 1,4-cyclodehydration of C4 diols, 1,4-butanediol and erythritol in water. Although HNbMoO_6 showed moderate activity for 1,4-butanediol dehydration, it exhibited the highest activity for erythritol dehydration, which followed a Tamaru mechanism with two successive irreversible steps. The larger value of the pre-exponential factor for erythritol over 1,4-butanediol can be ascribed to the larger mobility of the activated complex, due to the accessibility in the layered structure. Both 1,4-butanediol and erythritol were able to be intercalated into the interlayers of HNbMoO_6 , but the degree of expansion of the layers was different between the two C4 diols. The high activity of erythritol dehydration can be attributed to the increase of interlayer spacing.

Acknowledgements

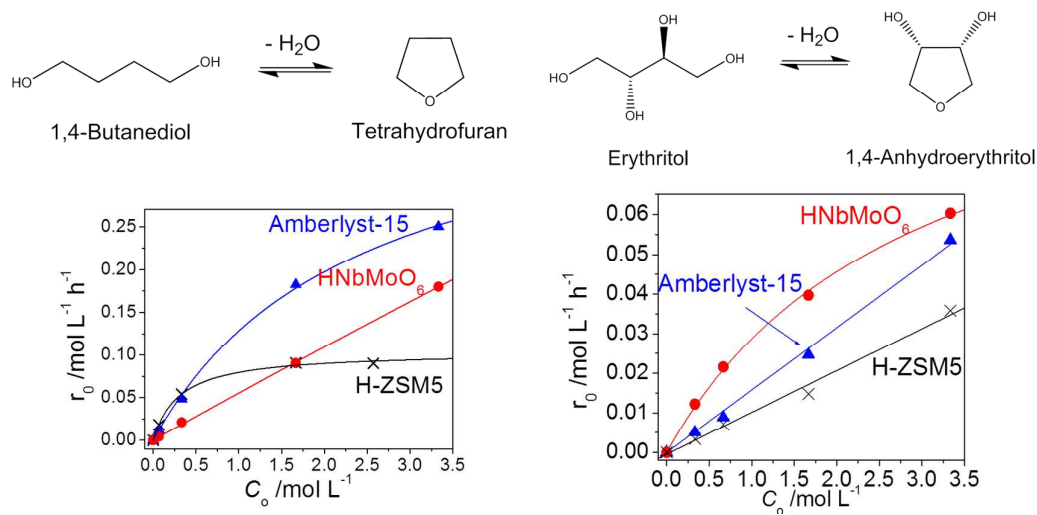
The author thanks Prof. S. Ted Oyama for valuable discussions. This work was supported by a Grant-in-Aid for Young Scientists (A) (No. 25709077) of MEXT, Japan, Tokuyama Science Foundation, Japan and Companhia Brasileira de Metalurgia e Mineração (CBMM), Brazil.

Notes and references

- S. Namba, N. Hosonuma and T. Yashima, *J. Catal.*, 1971, **72**, 16.
- A. Corma and M. Renz, *Chem. Commun.*, 2004, 550.
- M. Toda, A. Takagaki, M. Okamura, J.N. Kondo, S. Hayashi, K. Domen and M. Hara, *Nature*, 2005, **438**, 178.
- J. Ji, G. Zhang, H. Chen, S. Wang, G. Zhang, F. Zhang and X. Fan, *Chem. Sci.*, 2011, **2**, 484.
- K. Nakajima, Y. Baba, R. Noma, M. Kitano, J.N. Kondo, S. Hayashi and M. Hara, *J. Am. Chem. Soc.*, 2011, **133**, 4224.
- Y. Wang, F. Wang, Q. Song, Q. Xin, S. Xu and J. Xu, *J. Am. Chem. Soc.*, 2013, **135**, 1506.
- K. Inumaru, T. Ishihara, Y. Kamiya, T. Okuhara and S. Yamanaka, *Angew. Chem., Int. Ed.*, 2007, **46**, 7625.
- Y. Liu, K. Mo and Y. Cui, *Inorg. Chem.*, 2013, **52**, 10286.
- L. Vilcocq, P.C. Castilho, F. Carvalheiro and L.C. Duarte, *ChemSusChem*, 2014, **7**, 1010.
- R. Gounder and M.E. Davis, *J. Catal.*, 2013, **308**, 176.
- C. García-Sancho, I. Sádaba, R. Moreno-Tost, J. Mérida-Robles, J. Santamaría-González, M. López-Granados and P. Maireles-Torres, *ChemSusChem*, 2013, **6**, 635.
- T. Imai, T. Satoh, H. Kaga, N. Kaneko and T. Kakuchi, *Macromolecules*, 2004, **37**, 3113.
- M. Rose and R. Palkovits, *ChemSusChem*, 2012, **5**, 167.
- N.S.P. Bhuvanesh and J. Gopalakrishnan, *Inorg. Chem.*, 1995, **34**, 3760.
- C. Tagusagawa, A. Takagaki, S. Hayashi and K. Domen, *J. Am. Chem. Soc.*, 2008, **130**, 7230; C. Tagusagawa, A. Takagaki, K. Takanabe, K. Ebitani, S. Hayashi and K. Domen, *J. Phys. Chem. C*, 2009, **113**, 17421.
- Y. Morita, S. Furusato, A. Takagaki, S. Hayashi, R. Kikuchi and S.T. Oyama, *ChemSusChem*, 2014, **7**, 748.
- M.A. Harmer and Q. Sun, *Appl. Catal. A: Gen.*, 2001, **221**, 45.
- M. Boudart, C. Egawa, S. T. Oyama and K. Tamaru, *J. Chim. Phys.*, 1981, **78**, 987.
- K. Tamaru, *Acc. Chem. Res.*, 1988, **21**, 88.
- A. Vannice, *Kinetics of Catalytic Reactions*, Springer Science, New York, NY 2005, p. 110
- "Entropy and Heat Capacity of Organic Compounds" by Glushko Thermocenter, Russian Academy of Sciences, Moscow in NIST Chemistry WebBook, NIST Standard Reference Database Number 69, Eds. P.J. Linstrom and W.G. Mallard, National Institute of Standards and Technology, Gaithersburg MD, 20899, <http://webbook.nist.gov>, (retrieved November 3, 2014).
- M. S. Kelkar, J. L. Rafferty, E. J. Maginna and J. I. Siepmann, *Fluid Phase Equilibria*, 2007, **260**, 218.
- A. J. Lopes Jesus, M. T. S. Rosado, I. Reva, R. Fausto, M. Ermelinda, S. Eusébio and J. S. Redinha, *J. Phys. Chem. A*, 2008, **112**, 4669.
- The relatively large difference between experimental and calculated pre-exponential factors could be attributed to the treatment of Arrhenius plot in which large slope (E_a/R) causes y-intercept ($\ln A$) with high deviation.
- T. Bligaard, K. Honkala, A. Logadottir, J.K. Nørskov, S. Dahl and C.J.H. Jacobsen, *J. Phys. Chem. B*, 2003, **107**, 9325.
- D. Teschner, G. Novell-Leruth, R. Farra, A. Knop-Gericke, R. Schlögl, L. Szentmiklósi, M. González Hevia, H. Soerijanto, R.

- Schomäcker, J. Pérez-Ramírez and N. López, *Nat. Comm.*, 2012, 4, 739.
- 27 D. H. Olson, G.T. Kokotailo and S. L. Lawton, *J. Phys. Chem.*, 1981, **85**, 2238.
- 28 M. Aghaziarati, M. Kazemeini, M. Soltanieh and S. Sahebdehfar, *Ind. Eng. Chem. Res.*, 2007, **46**, 726.
- 29 U. Costantino, R. Vivani, V. Zima, L. Beneš and K. Melanová, *Langmuir*, 2002, **18**, 1211.

Graphical Abstract



HNbMoO₆ exhibited the highest activity for erythritol dehydration, which followed a Tamaru mechanism with two successive irreversible steps.